High-Flux Heat Transfer Characteristics of Pure Ethylene Glycol in Axial and Swirl Flow

W. R. GAMBILL and R. D. BUNDY

Oak Ridge National Laboratory, Oak Ridge, Tennessee

Measurements were made of heat transfer rates and peak heat flux for atmospheric-pressure pool boiling, and of adiabatic and diabatic friction factors, nonboiling and local-boiling heat transfer rates, and burnout heat fluxes for both axial- and twisted-tape swirl-flow forced convection of pure ethylene glycol. Test sections were electrically heated copper, 347 stainless steel, and A-nickel tubes.

Both axial- and swirl-flow friction factors are in good agreement with available generalized correlations. At the higher Reynolds numbers and heat fluxes axial-flow nonboiling heat transfer coefficients show a dependence of Nusselt number on $N_{Re}^{0.98}$ rather than the traditional $N_{Re}^{0.80}$. Swirl-flow nonboiling heat transfer coefficients from both the glycol data and previously obtained water data are satisfactorily correlated by a single equation. Nucleate-boiling heat transfer coefficients for both ethylene glycol and water fall approximately 50% above Kutateladze's suggested average line. The atmospheric-pressure pool-boiling peak flux is 168,000 Btu/hr. sq. ft. Forced-convection burnout heat fluxes are correlated in a number of ways, including a new additive method which appears to be generally applicable to a large variety of coolants, geometries, and flow conditions.

In order to gain a more complete understanding of the influence of physical properties on swirl-flow heat transfer, which has been studied at Oak Ridge National Laboratory with water as coolant (*1*), a swirl-flow study of ethylene glycol was initiated. The program was broadened to finally encompass the pool boiling, forced-convection nonboiling and local boiling, and burnout characteristics of ethylene glycol in both axial and swirl flow. A few tests were made under cooling conditions. The present paper is a summary of this investigation.

EXPERIMENTAL SYSTEM

The system used was basically the same as that used for the water studies (*1*). Moyno and turbine pumps were used singly or together to pump the glycol through horizontal copper or 347 stainless steel test sections, resistance heated by 60 cycle/sec. a.c. current. The glycol was contained in a mixed overhead holdup drum which could be steam heated or water cooled with internal coils. A cooler tube, which followed the heater tube in some tests, was externally jacketed to form an annular flow passage for longitudinal flow of cooling water; 40-gauge (3-mil-diam.) chromel/alumel thermocouples were embedded in the cooler tube wall. An upstream calming section longer than 40 diam. was used in all axial-flow tests. Swirl flow was generated with thin (15 mil thick) twisted tapes, onto which the tubes were drawn, as described in reference *1*.

Burnout tests were concluded by physical destruction of the test section (usually near the flow exit). Burnout was attained by slowly increasing the heat flux at essentially constant velocity, pressure, and inlet glycol temperature.

The pool boiler, which measured nominally 6 by 6 by 9 in. deep, was similar to that used by Averin(*2*). The horizontal heater tube was silver soldered across two insulated copper end plates which served as electrodes; the bottom and sides were made of welded stainless-steel plate. Thermocouples (chromel/alumel in all tests) were placed inside the heater tube and longitudinal traverses made under heating conditions to determine the location of the isothermal zone. External silver voltage leads and the four internal thermocouples were then located within this zone.

PHYSICAL PROPERTIES

Three analyses of the glycol in the loop were made during the tests; the composition ranged from 99.6 to 99.8 wt. % glycol (balance water). Values for specific heat, liquid density, latent heat of vaporization, thermal conductivity, and viscosity were taken from a supplier bulletin (*3*) and from Curme and Johnston (*4*). Surface tension was obtained from Lange (*5*), the critical temperature and pressure were estimated with Eduljee's additive-contribution method (*6*), vapor density was calculated from the gas law with compressibility factors from the Pitzer-Edmister charts (*7*), and β was calculated from available liquid-density data. Some extrapolation of property values was necessary, especially for surface tension and latent heat of vaporization; some uncertainties consequently exist for the glycol property data over the temperature range of interest. Table 1 is a tabulation of the physical-property values used, which were taken from best curves through the data. No glycol decomposition or wall deposition was noted, so fluid properties were considered time independent.

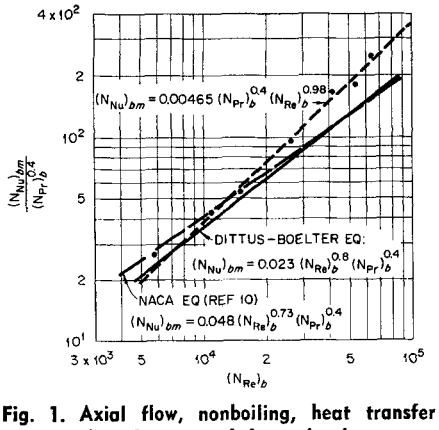

Fig. 1. Axial flow, nonboiling, heat transfer data for pure ethylene glycol.

FRICTION FACTORS

Nine isothermal friction factors measured for axial flow of glycol through a ¼-in.-I.D. tube deviated by 2.1% average and 4.8% maximum from the standard Moody curve (*8*) for the same relative roughness. The Reynolds number range in these tests was 4.5×10^3 to 7.5×10^4.

Isothermal friction factors measured for swirl flow of glycol were in reasonable agreement with a generalized swirl-flow friction-factor correlation developed from water and air data (*9*):

$$(f_s - f_a)_{s,\,iso} = \frac{0.21}{y^{1.81}}\left[\frac{(N_{Re})_s}{2{,}000}\right]^{-n} \tag{1}$$

where

$$n = 0.81 \exp\left[-1{,}700\,(\epsilon/D_e)\right] \tag{1a}$$

Values calculated from Equation (1) deviated by a maximum of 16.5% from the mean lines through the data for swirl flow of glycol through ¼-in.-I.D. tubes with $y = 4.8$ over the range

2.5 by $10^3 < (N_{Re})_a < 9.5$ by 10^4.

Swirl-flow friction factors measured with 0.136- and ¼-in.-I.D. tubes under heating (nonboiling), and cooling conditions were correlated with about the same accuracy by inclusion of the wall-to-bulk viscosity ratio:

$$f/f_{iso} = (\mu_w/\mu_b)^{n'} \tag{2}$$

The exponent n' for the cooler data at $y = 4.8$ was considerably smaller (0.043) than for the heater data, for which n' was found to vary with the tape-twist ratio according to

$$n' = 0.140 - \frac{0.3465}{y^2} \tag{3}$$

over the range $2.26 < y < \infty$.

A fully detailed description of this work will be given in an Oak Ridge National Laboratory report of the same title issued in 1963.

TABLE 1. PHYSICAL PROPERTIES OF ETHYLENE GLYCOL*

Property	t, (°C.) 20	50	100	150	200	250	300
$(c_p)_l$, B.t.u./lb. °F.	0.560	0.595	0.653	0.712	0.769	0.827	—
μ_l, lb./ft. sec. $\times 10^3$	14.7	4.9	1.45	0.60	0.28	0.13	0.053
k_l, B.t.u./hr. ft. °F.	0.168	0.154	0.133	0.109	0.086	0.071	0.061
$(N_{Pr})_l$	157	68	26.2	15.4	11.8	—	—
ρ_l, lb./cu. ft.	69.50	68.22	65.92	63.23	60.38	54.37	45.25
$(\rho_v)_{sat}$, lb./cu. ft.	—	—	—	—	0.123	0.776	6.31
p^*, lb./sq. in. abs.	0.00097	—	—	—	17.8	114	510
λ, B.t.u./lb.	—	—	—	409	374	322	249
σ, dynes/cm.	47.7	45.4	40.0	33.2	25.6	17.5	8.9
β_l, $(°C)^{-1} \times 10^3$	0.626	0.654	0.773	0.894	1.015	—	—

* $C_2H_4(OH)_2$, $M = 62.1$. Normal boiling point = 197.5°C. Freezing point = −13.0°C. Estimated critical properties: T_c = 1,133°R. = 629°K.; P_c = 1,043 lb./sq. in. abs. = 71.0 atm. abs.

NONBOILING HEAT-TRANSFER COEFFICIENTS

Axial Flow

In a previous study Bernardo and Eian (*10*) correlated their data for ethylene glycol and its aqueous solutions, in addition to comparative data for water and *n*-butanol, by the equation

$$(N_{Nu})_{bm} = 0.048\ (N_{Re})_b^{0.73}\ (N_{Pr})_b^{0.4} \qquad (4)$$

For the purest glycol tested (AN-E-2 grade, 94.5 wt. % glycol) the tests of reference *10* were conducted at moderate Reynolds numbers, 5.0 by $10^3 < (N_{Re})_b < 3.15$ by 10^4, and at very low heat fluxes, 0.035 by 10^6 B.t.u./hr. sq.ft. maximum.

The nonboiling tests of the present investigation were conducted at higher Reynolds numbers (up to 63,000) and at much higher heat fluxes (2.40 by 10^6 B.t.u./hr.-sq.ft. maximum). The results are shown in Figure 1, wherein the glycol data are correlated within average and maximum deviations of 7.3 and 17.8% by

$$(N_{Nu})_{bm} = 0.00465\ (N_{Re})_b^{0.98}\ (N_{Pr})_b^{0.4} \qquad (5)$$

At $N_{Re} < 10^4$ Equation (5) tends to underestimate the Nusselt number, and a curved or two-segment line, coinciding with the National Advisory Committee for Aeronautics line at low Reynolds numbers, would probably give a better overall representation. It was at first thought that the result expressed by Equation (5) was in error, but a very extensive check of the system (rotameters, thermocouples, instruments, and heat generation external to the test section) confirmed the validity of the data. It was subsequently learned that similar studies at Rocketdyne with organic liquids flowing at high velocities and under large impressed heat fluxes also consistently gave a Reynolds number exponent larger than the traditional 0.8. For RP-1 fuel (kerosene) for example the Rocketdyne data were best correlated by (*11*) $(N_{Nu})_b \propto (N_{Re})_b^{0.95}$, for diethylcyclohexane by (*11*) $(N_{Nu})_b \propto (N_{Re})_b^{0.93}$, and for hydrazine by (*12*) $(N_{Nu})_b \propto (N_{Re})_b^{0.98}$. It may also be noted that the present results are correlated within an average deviation of ± 16.5% by the extended analogy of Friend and Metzner (*24*), which predicts a variable Reynolds number exponent.

Such results may be explained in part by the variation of the friction factor with Reynolds number. The Colburn type of analogy

$$N_{Nu}/N_{Pr}^{1/3} = (f/8)\ N_{Re} \qquad (6)$$

gives the usual variation of Nusselt number with $N_{Re}^{0.8}$ only when $f/8$ is correlatable by the average and Reynolds number-limited relation $f/8 = 0.023/N_{Re}^{0.2}$. At low wall Reynolds numbers, as in the National Advisory Committee for Aeronautics tests (*10*), the friction-factor curve is steeper and the Reynolds number exponent < 0.8, whereas at high wall Reynolds numbers, as in this study, the friction-factor curve is flatter and the Reynolds number exponent > 0.8. By wall Reynolds number is meant a Reynolds number evaluated with physical properties taken at the wall (or film) temperature. Such a Reynolds number appears more pertinent in the subject case, which is characterized by a large radial contrast of fluid properties, especially of viscosity. In addition extreme gradients in the radial temperature and velocity profiles caused by the combination of high heat fluxes and a large Prandtl number could be sufficient to render the normal Nusselt number correlations inadequate.

Swirl Flow

The glycol data were first compared with the earlier correlation developed for swirl-flow water (*1*), that is a log-log plot of h_{sm}/h_{am} vs. $(N_{Gr}/N_{Re}^2)_a \propto (\beta \Delta t)_f^{1/2}/y$, where h_{am} is calculated from

$$h_{am} = \frac{0.023\ c_{pb}\ G\ [1 + (D_i/L_h)^{0.7}]}{(N_{Pr})_b^{2/3}\ (N_{Re})_b^{0.2}} \qquad (7)$$

This correlation procedure gave a mean line through the glycol heating data (8.9% average deviation for sixty-five points) which fell ~ 30%

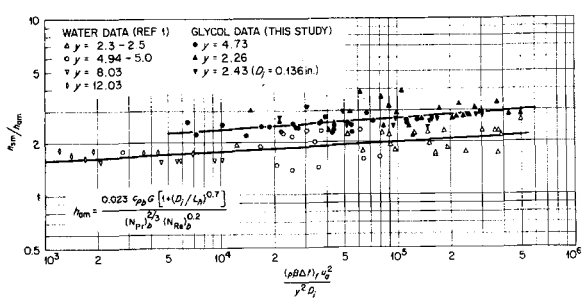

Fig. 2. Swirl flow heat transfer data, heating (ethylene glycol and water).

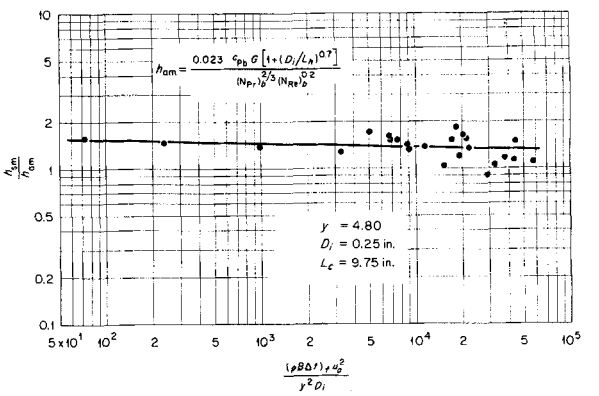

Fig. 3. Swirl flow heat transfer data, cooling (ethylene glycol).

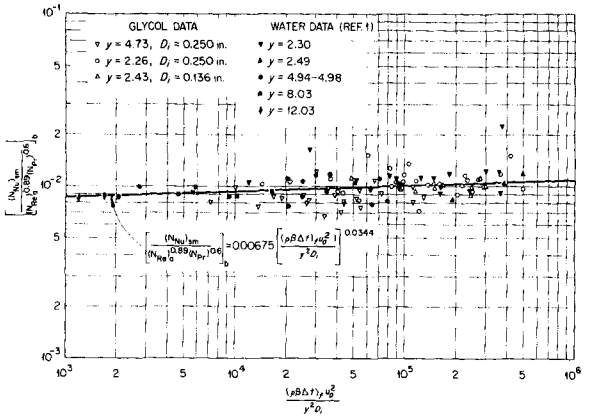

Fig. 4. Swirl flow heat transfer data, heating (ethylene glycol and water).

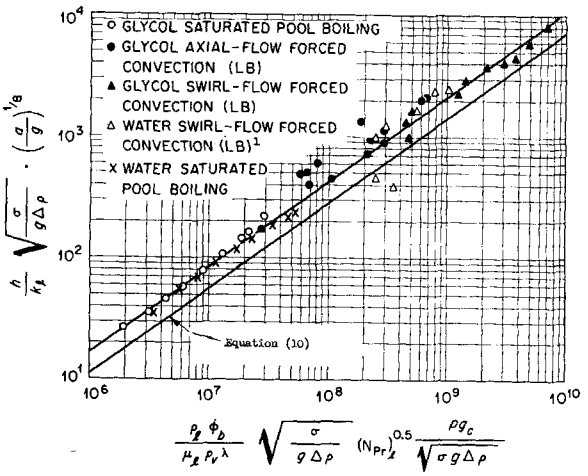

Fig. 5. Combined nucleate boiling heat transfer data, ethylene glycol and water.

above the water line. Eight check tests with water at $y = 4.73$ were within $+7\%$ of the original line (*1*). The twenty-four cooling points did not correlate, giving a broad scatter of h_{sm}/h_{am} over a narrow range of $(N_{Gr}/N_{Re}^2)_a$. If Equation (5) rather than Equation (7) is used for calculating h_{am} for glycol, the glycol curve is lowered into better agreement with the earlier water data at large values of $(N_{Gr}/N_{Re}^2)_a$ but with no improvement at small values, where the glycol data now fall below rather than above the water line.

The swirl-flow heat transfer coefficient data may also be correlated on the basis of buoyant force per unit fluid volume, that is with

$$F_b/v = \frac{\pi^2 (\rho \beta \Delta t)_f u_a^2}{2 y^2 D_i g_c} \propto \frac{(\rho \beta \Delta t)_f u_a^2}{y^2 D_i} \qquad (8)$$

Results for heating are given in Figure 2, where the average deviations for the water and glycol data are 11.7 and 8.9%, respectively, and for cooling in Figure 3 (13.2% average deviation). The cooling data may be expected to scatter more since the bulk-temperature changes were generally much smaller than in the heating tests. The buoyant-force correlation of Figures 2 and 3 indicates that h_{sm}/h_{am} increases with liquid-film temperature gradient and centrifugal intensity with heating, but decreases with cooling. This is reasonable since with heating, buoyant forces remove hotter fluid from the wall, while with cooling the same forces act to keep the cooler, denser fluid on the wall. The heat transfer coefficient ratio is still > 1 with cooling however, probably because of enhanced turbulence with swirl flow.

All of the glycol and water swirl-flow heating data were correlated by a single line, as shown in Figure 4, by plotting $(N_{Nu})_{sm}/N_{Re}^{s} N_{Pr}^{t}$ vs. F_b/v. Average exponents were determined by separate cross plotting to be $s = 0.89$ and $t = 0.6$. In previous correlations the Prandtl number exponent had been assumed to be 0.4 in the Nusselt form or 2/3 in the Colburn form. The resulting correlation

$$\left[\frac{(N_{Nu})_{sm}}{(N_{Re})_a^{0.89}(N_{Pr})^{0.6}}\right]_b = 0.00675 \left[\frac{(\rho \beta \Delta t)_f u_a^2}{y^2 D_i}\right]^{0.0344} \qquad (9)$$

fits the 103 points of Figure 4 within an average deviation of $\pm 12.0\%$. The dimensional group on the right side of Equation (9) and in Figures 2 to 4 should be evaluated in units of pounds per cubic foot, feet per second, and feet.

Koch (*13*) hypothesized that the heat transfer enhancement associated with various types of turbulator tube inserts, including twisted tapes, is caused by an increased turbulent intensity, fluids of small Prandtl number benefiting the most. The 0.6 Prandtl number exponent of Equation (9) suggests, on the contrary, that the improvement is greatest for fluids with a high thermal resistance near the wall (large Prandtl number), and that buoyant action can be more important in swirl flow than increased turbulence. This does not imply however that turbulence intensification is not a factor in swirl flow, since even with cooling the heat transfer coefficient ratio is still generally > 1. Further experiments will be required to determine the relative contributions of turbulence and of buoyant action.

NUCLEATE-BOILING HEAT-TRANSFER COEFFICIENTS

Pool-Boiling Tests

Pool tests were conducted with glycol and water outside horizontal A-nickel tubes (¼ in. by 35-mil wall by 6 in. long) at a pressure of 739-mm. mercury (plus ~3-in. liquid head). Average initial and after-test root mean square external surface roughnesses were 39 and 53 μin., respectively. The results are given in Table 2. The precision of the data in these tests was $\pm 5\%$ average, with respect to heat flux, for all the points.

Overall Correlation

The glycol and water pool-boiling data were combined with the forced-convection data for water and glycol and reduced in accordance with Kutateladze's dimensionless nucleate-boiling equation (*14*), as described by Zuber and Fried (*15*):

$$\frac{h}{k_l}\left(\frac{\sigma}{g \Delta \rho}\right)^{0.5} = (7.0 \times 10^{-4}) \times \left[\frac{\rho_l}{\mu_l} \frac{\phi_b}{\lambda \rho_v} \sqrt{\frac{\sigma}{g \Delta \rho}}\right]^{0.7} \times$$

Table 2. Atmospheric-Pressure Saturated Pool-Boiling Test Results

Fluid	Number points	Isothermal zone	Δt_{sat}, °F.	Slope*	At boiling transition† ϕ_{bo}	$(\Delta t_f)_{bo}$	h_{bo}
Distilled water, this study	24	0.76 L_h	17.6-43.0	2.4-3.6	485,000	43.0	11,400
Distilled water, Averin (2)	—	—	—	—	461,000	47.7	9,440
Pure ethylene glycol	9	0.56 L_h	27.7-49.9	3.8-5.9	168,000	49.9	3,380

* Slope of curve of heat flux vs. wall superheat.
† British thermal units, hours, feet, and degrees Fahrenheit.

$$\times (N_{Pr})_l^{0.85} \left[\frac{p\, g_o}{\sqrt{\sigma\, g\, \Delta\rho}}\right]^{0.7} \qquad (10)$$

The data fall about a line 51% above Kutateladze's suggested average line, as shown in Figure 5. The heat flux correlated is the boiling heat flux, that is total ϕ minus $(\phi)_{nb}$ calculated from Equations (5) and (9) for axial and swirl flow, respectively. Note that for nondimensionality with English engineering units the surface tension in Equation (10) and in Figure 5 must be expressed as pound-mass per hour squared.

To bring the swirl data into approximate agreement with the pool-boiling and axial-flow data it was necessary to introduce into Equation (10), as shown in Figure 5, the empirical factor $(a/g)^{0.125}$. Attainable superheats are larger with swirl flow than with axial flow, and $\Delta t^*_{sat} = \Delta t_{sat}/(a/g)^{0.125}$ was found to be of the same order as observed for pool boiling and axial flow. Unlike Rohsenow's correlation (*16*) Kutateladze's does not contain a constant which is adjustable for specific surface-fluid combinations, so that some nucleate-boiling data would be expected to deviate considerably from his average line.

BURNOUT HEAT FLUX

Pool Boiling

In the dimensionless Kutateladze equation for pool-boiling burnout (*14*)

$$(\phi_{bo})_{pool,\ sat} = K \lambda \rho_v \left[\frac{\sigma\, a\, \Delta\rho}{\rho_v^2}\right]^{1/4} \qquad (11)$$

Zuber maintains (*17*) that $0.120 < K < 0.157$. Available experimental data (*14, 18*) however give a maximum K range of 0.08 to 0.23. The K values for the water and glycol data of Table 2 are 0.182 and 0.121, respectively.

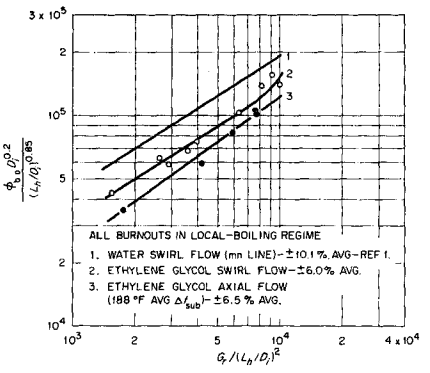

Fig. 6. Ethylene glycol burnout data compared with swirl flow burnout correlation for water.

Axial Forced Convection

All forced-convection burnout data are given in Table 3; test-section L/D ratios ranged from 29 to 102. Flash fires occurring at burnout discouraged further tests, since the facility was not designed to handle fires or explosions. The fires, which were of brief duration (a few seconds), were generally more severe with axial flow than with swirl flow.

The burnout correlations of Griffith (*19*) and of Bernath (*20*) predict values of burnout heat flux considerably lower (50% and more) than those observed. A new additive burnout method (*21*) also consistently predicts ~43% low; this result appears anomalous since the swirl glycol data are well correlated by this method, and some 900 other point comparisons with data taken from the literature are in much better agreement.

The axial burnout data may be empirically correlated with an equation of the type used by Gunther for low-pressure water (*22*) by altering only the coefficient:

$$(\phi_{bo})_a = 3{,}330\, u^{1/2}\, (\Delta t_{sub})_{bo}^{3} \qquad (12)$$

where u is in feet per second, Δt_{sub} in degrees Fahrenheit and ϕ in British thermal units per hour-square feet. Average and maximum deviations for Equation (12) are 13.5 and 21.6%. Since only five axial tests were made, a more refined empirical correlation would be valueless. The axial data are also plotted in Figure 6 (units of British thermal units, pounds, hours, and feet), which pertains primarily to swirl flow.

Swirl Forced Convection

In four of the swirl tests burnout occurred near the test-section inlet. This had never occurred previously during water swirl-flow burnouts; but since no upstream calming section is provided for the swirl test sections, it is believed that the greater viscosity and Prandtl number of the glycol did not allow the coolant flow to develop sufficiently before it was exposed to high heat fluxes. This explanation is supported to some extent by the fact that in three of the four inlet burnouts the tape-twist ratio and inlet-bulk temperature were small.

The Griffith (*19*) and Bernath (*20*) correlations generally gave, as with the water swirl burnout data (*1*), quite large deviations. The best correlation for the water data (*1*) was applied to the present results as shown in Figure 6. As noted in reference *1* swirl burnout fluxes appear to be nearly independent of subcooling.

A new additive prediction method (*21*) may be summarized as follows:

$$\phi_{bo} = \phi_b + \phi_{nb} \qquad (13)$$

where

$$\phi_b = [\text{Equation (11)}] \times \times \left[1 + (\rho_l/\rho_v)^{0.923} \left(\frac{c_p\, \Delta t_{sub}}{25\, \lambda}\right)\right] \qquad (14)$$

and

$$\phi_{nb} = h_{nb}\, (t_w - t_b)_{bo} \qquad (15)$$

The second bracketed term in Equation (14) is Kutateladze's empirical

TABLE 3. FORCED-CONVECTION BURNOUT TESTS WITH ETHYLENE GLYCOL

Test no.	Test section D_i, in.	Test section L_h, in.	Test section Material	y^*	$\bar{\epsilon}$, μin. root mean square†	t_{b_1}, °F.	p_{bo}, lb./sq. in. abs.**	$(u_a)_{bo}$, ft./sec.	$(t_{sat})_{bo}$, °F.	$(t_b)_{bo}$, °F.	$(\Delta t_{sub})_{bo}$, °F.	a/g, gees††	x_{bo} — L_h	(ϕ_{bo}),*** 10^{-6} B.t.u./hr. sq. ft.
1	0.249	11.91	Copper	4.73	17.7	138	41.0	25.4	427	337	90	212	0.96	3.68
2	0.249	11.88	Copper	2.26	24.3	72	279.0	72.0	536	117	419	7,510	0.26	9.00
3	0.136	13.81	Copper	2.43	63.3	148	140.0	63.2	493	416	77	9,190	0.96	5.32
4	0.249	11.98	Copper	7.73	43.3	73	170.0	38.0	506	80	426	178	0.04	4.38
5	0.249	11.98	Copper	11.81	27.9	127	43.9	62.3	431	264	167	204	0.96	5.99
6	0.249	11.98	Copper	12.10	20.4	98	20.4	35.0	398	259	139	62	0.96	3.97
7	0.249	11.98	Copper	12.05	27.5	115	33.3	97.5	418	234	184	484	0.96	8.11
8	0.249	11.98	Copper	7.74	21.5	73	19.9	28.2	397	252	96	98	0.96	3.42
9	0.249	11.98	Copper	2.18	22.7	145	27.1	66.8	408	311	97	6,940	0.96	8.03
10	0.249	11.98	Copper	No tape	32.9	124	19.5	17.3	396	240	156	1	0.96	2.06
11	0.249	12.94	Copper	No tape	29.6	127	31.7	88.4	415	234	181	1	0.89	6.25
12	0.249	12.10	Copper	No tape	37.8	149	31.4	60.2	415	260	155	1	0.96	4.89
13	0.249	7.25	347 ss	2.45	27.3	111	36.9	21.4	439	115	324	564	0.07	2.33
14	0.249	7.19	347 ss	2.38	28.2	103	64.2	30.6	450	108	342	1,221	0.07	3.40
15	0.249	11.98	Copper	No tape	25.8	124	87.7	67.3	467	203	264	1	0.66	6.23
16	0.249	11.90	Copper	No tape	†††	122	29.1	40.6	412	227	185	1	0.94	3.42

* Checked by x-ray measurements.
† Average value determined after test at 3 to 8 axial positions.
** All pressures are subcritical.
†† Calculated from equation based on rotating slug-flow model (*1*).
*** The local ϕ_{bo} at the burnout site, which is the value listed, differed from the tube-average ϕ_{bo} by <5% in all cases.
††† Not measured.

dimensionless subcooling factor for pool-boiling burnout (23), and $(t_w)_{bo}$ in Equation (15) is evaluated with Bernath's generalized graph (20) of $(\Delta t_{sat})_{bo}$ vs. T_{sat}/T_c. The specific heat is evaluated at the reference temperature t'. This method, which is an extension to the burnout condition of Rohsenow's additive technique for local-boiling heat transfer rates below burnout (16), correlates nine of the glycol burnouts (two inlet burnouts omitted) within average and maximum deviations of 12.5 and 39.3% when K is taken as 0.16 and h_{sm} evaluated with the glycol data of this study.

GENERAL CONCLUSIONS

1. Equation (1) appears to be adequate for predicting isothermal friction factors for a variety of fluids in swirl flow.

2. Organic fluids, and perhaps water, give larger nonboiling axial-flow heat transfer coefficients at high velocities and heat fluxes than predicted by standard correlations. For such conditions the Reynolds number exponent appears to be nearer 1.0 than 0.8.

3. Use of F_b/v gives a better overall correlation of heating and cooling swirl-flow heat transfer coefficient data than does $(N_{Gr}/N_{Re}^2)_a$. Equation (9) adequately correlates all available Oak Ridge National Laboratory swirl-flow heating data.

4. With saturated pool boiling, axial forced-convection local boiling, and swirl forced-convection local boiling, respectively, ethylene glycol is characterized, for the variable ranges of this study, by burnout heat fluxes ~ 1/3, 1/2, and 3/4 those for water at the same conditions of geometry, velocity, pressure, and bulk temperature.

ACKNOWLEDGMENT

The authors wish to express their appreciation to Joseph Lones and D. H. Wallace for their able assistance as project technicians, and to Dolores Eden for her conscientious typing of the manuscript.

NOTATION

a = local acceleration
c_p = constant-pressure specific heat of fluid
D = flow-passage diameter
f = Darcy friction factor, $2\,g_c D_i \Delta p/u_a^2 L_a \rho_b$, dimensionless
F_b/v = buoyant force per unit fluid volume
g = local gravitational acceleration
g_c = conversion constant, $L \cdot M/\theta^2 \cdot F$
G = mass velocity of fluid, ρV
N_{Gr} = Grashof number, $D^3 \rho^2 a \beta (\Delta t)_f/\mu^2$, dimensionless
G_r = resultant mass velocity of fluid, ρV_r
h = surface heat-transfer coefficient
k = thermal conductivity of fluid
K = constant in Equation (11)
L = length of test section
LB = local boiling
M = molecular weight
n, n', s, t = exponents
N_{Nu} = Nusselt number, hD/k_l, dimensionless
N_{Pr} = Prandtl number, $c_p\mu/k$, dimensionless
N_{Re} = Reynolds number, $D\,G/\mu_l$, dimensionless
p = absolute pressure
p^* = absolute vapor pressure
Δp = pressure drop
t = temperature
t' = reference temperature, $t_{sat} - (\Delta t_{sub}/2)$
T = absolute temperature
Δt_f = film temperature change, $(t_w - t_b)$ or $(t_b - t_w)$
Δt_{sat} = wall superheat, $(t_w - t_{sat})$
Δt_{sub} = degree of subcooling, $(t_{sat} - t_b)$
u = velocity of fluid
x_{bo} = distance from heated inlet to burnout site
y = tape-twist ratio, inside diameters per 180-deg. twist

Greek Letters

β = volumetric coefficient of thermal expansion of fluid
ϵ = mean root mean square height of surface roughness elements
λ = latent heat of vaporization of coolant
μ = dynamic viscosity of fluid
ρ = density of fluid
$\Delta\rho$ = phase density difference, $(\rho_l - \rho_v)$
σ = surface tension of liquid
ϕ = heat flux into fluid

Subscripts

a = axial flow; based on D_i and u_a
b = bulk coolant, boiling contribution
bo = burnout value; at burnout site
c = critical; cooled
e = equivalent; based on D_e and u_a
f = at arithmetic-average film temperature
h = heated
i = internal
iso = isothermal
l = liquid
m = mean
nb = nonboiling
r = resultant value
s = swirl flow
sat = saturation value
v = vapor
w = at wall
1 = at test-section inlet

LITERATURE CITED

1. Gambill, W. R., R. D. Bundy, and R. W. Wansbrough, *Chem. Eng. Progr. Symposium Ser., No. 32*, **57**, 127-137 (1961). Fully reported by same authors in *Oak Ridge Natl. Lab. Report 2911* (March 28, 1960).
2. Averin, E. K., *Izvest. Akad. Nauk, SSSR*, No. 3, 116-122 (1954); available as *Atomic Energy Research Establ. Lib/Transl. 562* (1955).
3. Union Carbide Chemicals Company data folder, *Ethylene Glycol* (September, 1956).
4. Curme, G. O., Jr., and Franklin Johnston, ed., "Glycols," Am. Chem. Soc. Monograph 114, Reinhold, New York (1952).
5. Lange, N. A., ed., "Handbook of Chemistry," 7 ed., p. 1614, Handbook Publishers, Sandusky, Ohio (1949).
6. Gambill, W. R., *Chem. Eng.*, 181-184 (June 15, 1959); 157-160 (July 13, 1959).
7. Edmister, W. C., *Petrol. Refiner*, 173-179 (April, 1958).
8. Moody, L. F., *Trans. Am. Soc. Mech. Engrs.*, **66**, 671-684 (1944).
9. Gambill, W. R., and R. D. Bundy, *Oak Ridge Natl. Lab. CF Memo 61-4-61* (Unclass.) (April 24, 1961); *Am. Soc. Mech. Engrs. Paper No. 62-HT-42* (Aug., 1962).
10. Bernardo, E., and C. S. Eian, *Natl. Advisory Comm. Aeronaut. Wartime Report ARR No. E5F07* (Aug., 1945).
11. Hines, W. S., and J. D. Seader, *Rocketdyne Final Tech. Rept. (1960) G.O. 5038, RM 752/352* (January 20, 1961).
12. Hines, W. S., *Rocketdyne Rept. R-2059* (Declass.), (August 24, 1959).
13. Koch, R., *VDI—Forschungsheft*, Series B, **24**, No. 469, pp. 1-44 (1958).
14. Kutateladze, S. S., "Heat Transfer in Condensation and Boiling, 2 ed., Chapt. 10, Moscow—Leningrad (1952); *AEC Transl. 3770* (Aug., 1959).
15. Zuber, Novak, and E. Fried, Am. Rocket Soc. Paper No. 1709-61 (April, 1961).
16. Rohsenow, W. M., "Heat Transfer *Symposium, 1952,*" pp. 101-149, Engineering Research Institute, University of Michigan, Ann Arbor, Michigan (1953).
17. Zuber, Novak, Thesis, Univ. Calif., Los Angeles, California (June, 1959).
18. Borishanskii, V. M., *Zhurn. Tekh. Fiz.*, **25**, 252 (1956).
19. Griffith, P., Paper presented at Am. Soc. Mech. Engrs., First National Heat Transfer Conference, University Park, Pennsylvania (August, 1957).
20. Bernath, Louis, *Chem. Engr. Progr. Symposium Ser., No. 30*, **56**, 95-116 (1960).
21. Gambill, W. R., *Chem. Eng. Progr. Symposium Ser. No. 42*, **59** (1963). Also see W. R. Gambill and H. W. Hoffman, Am. Rocket Soc. paper No. 1737-61, Am. Rocket Soc.-Am. Nuclear Soc. Conference, Gatlinburg, Tennessee (May, 1961).
22. Gunther, F. C., *Trans. Am. Soc. Mech. Engrs.*, **73**, 115-123 (1951).
23. Kutateladze, S. S., *Izvest. Akad. Nauk, SSSR*, Otd. Tekh Nauk, No. 4, 529-536 (1951); also see C. F. Bonilla, "Nuclear Engineering," Ch. 9, p. 404, McGraw Hill, New York (1957).
24. Friend, W. L., and A. B. Metzner, *A.I.Ch.E. Journal*, **4**, No. 4, pp. 393-402 (1958).

Manuscript received February 28, 1962; revision received June 8, 1962; paper accepted June 12, 1962. Paper presented at A.I.Ch.E. Los Angeles meeting.